

Electronic structure and properties of isorecticular metal-organic frameworks: The case of *M*-IRMOF1 (*M*=Zn, Cd, Be, Mg, and Ca)

Miguel Fuentes-Cabrera,^{a)} Donald M. Nicholson, and Bobby G. Sumpter
 Computer Science and Mathematics Division, Oak Ridge National Laboratory, Oak Ridge,
 Tennessee 37831-6164

Mike Widom
 Department of Physics, Carnegie Mellon University, Pittsburgh, Pennsylvania 15213

(Received 4 May 2005; accepted 26 July 2005; published online 29 September 2005)

We investigate the possibility of tailoring the electronic properties of isorecticular metal-organic materials by replacing the metal atom in the metal-organic cluster and by doping. The electronic structure of *M*-IRMOF1, where IRMOF1 stands for isorecticular metal-organic framework 1 and *M*=Be, Mg, Ca, Zn, and Cd, was examined using density-functional theory. The results show that these materials have similar band gaps (ca. 3.5 eV) and a conduction band that is split into two bands, the lower of which has a width that varies with metal substitution. This variation prompted us to investigate whether doping with Al or Li could be used to tailor the electronic properties of the Zn-IRMOF1 and Be-IRMOF1 materials. It is shown that replacing one metal atom with Al can effectively be used to create IRMOFs with different metallic properties. On the other hand, adding Li produces structural changes that render this approach less suitable. © 2005 American Institute of Physics. [DOI: 10.1063/1.2037587]

I. INTRODUCTION

Porous metal-organic frameworks (MOFs) have emerged as a class of materials with enormous potential in a variety of practical applications. For example, MOFs can act as storage materials for hydrogen^{1,2} and methane,³ or they can be used as sensors,⁴ serve as templates for the creation of molecular species architectures,^{5,6} and perform enantioselective catalysis and separation.⁷ Additionally, chemists are finding ways to design MOFs to target specific properties.

Eddaoudi *et al.* have shown that porous MOFs can be synthesized as to target the capability to store hydrogen and methane: They used the reticular approach to synthesize 16 different MOFs with the same underlying topology but different chemical functionality of the pores;³ functionalizing the pores allows for different hydrogen and methane storage capabilities.¹ Here, we wish to investigate whether a similar concept can be used to target the electronic properties of these materials. As a first step, we concentrate on the material known as isorecticular metal-organic framework (IRMOF1).

The structure of IRMOF1 is shown in Fig. 1(a). The structure can be viewed as made of two distinct structural units, the connector [shown in Fig. 1(b)] and the linker [shown in Fig. 1(c)]. If one was to alter the electronic properties of IRMOF1, the following three approaches seem plausible: (i) replacing the linker with other organic molecules, (ii) replacing the connector by changing the metal atom in it, and (iii) replacing both the linker and connector.

Replacing the linker has already been done. In fact, IRMOF1 belongs to the class of 16 different IRMOFs men-

tioned above, all of them with the same connector and underlying topology but different linkers. Replacing Zn by other metal atoms can also be done, and this is the approach we chose here.

In selecting metal atoms that could replace Zn, it is convenient to choose those that are likely to form a Zn-acetate-type molecule, because this molecule plays a crucial role in the synthesis of IRMOFs.^{1,2} Be and Co are the most appropriate choices, since both form an acetate molecule,^{8,9} and the compounds Be-IRMOF1 and Co-IRMOF1 could most likely be synthesized. But Co is magnetic, and Co-IRMOF1 should have distinct properties that deserve a whole separate study. This led us to investigate IRMOF1 with Be, Zn, and similar atoms, including Mg, Ca, and Cd.

In what follows, we used an *ab initio* technique to investigate the electronic properties of *M*-IRMOF1, where *M*=Be, Mg, Ca, Zn, and Cd. Our results show that all of these materials have very similar large band gaps, with a conduction band of varying width. The latter finding suggested that it might be possible to dope these materials in order to raise the Fermi level up to conduction band. If so, one could take advantage of the variation in the width of the conduction band to create IRMOFs with different metallic properties. This idea is examined in detail by doping with Al and Li the materials Zn-IRMOF1 and Be-IRMOF1.

II. METHOD

The Vienna *ab initio* simulation package (VASP) code was used to perform the electronic structure calculations.¹⁰ The method is based on the local-density approximation (LDA) to the density-functional theory with ultrasoft Vanderbilt-type pseudopotentials.¹¹ The LDA used is of the Ceperly–Alder form¹² as parametrized by Perdew and

^{a)}Electronic mail: fuentescabma@ornl.gov

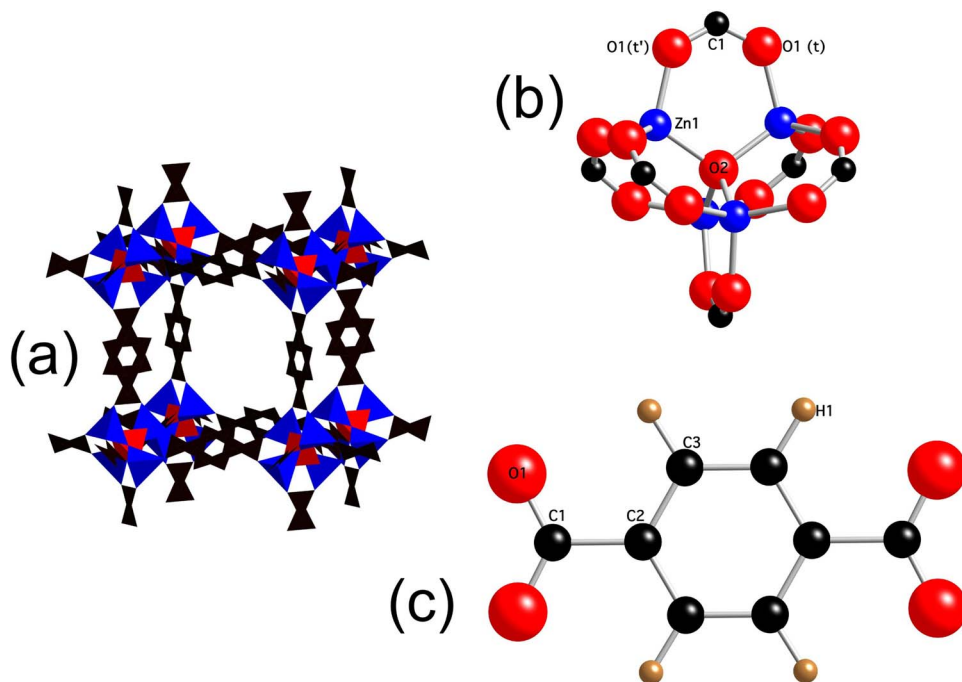


FIG. 1. The structure of IRMOF1. The labels C1, C2, etc., denote different crystallographic positions (see Table II). (a) A single cube fragment of the complete structure. Each corner of the cube is made up of a *connector*, and each side is made up of a *linker*. (b) Connector: it can be described as one central $(\text{Zn}1)_4(\text{O}2)$ tetrahedron and four $\text{Zn}1(\text{O}1)_3\text{O}2$ distorted tetrahedra; the labels $\text{O}1(t)$ and $\text{O}1(t')$ denote O1 atoms belonging to two different distorted tetrahedra. (c) Linker: reminiscent of the organic molecule 1,4 benzenedicarboxylate (BDC). In *M*-IRMOF1, two different linkers are connected to each other by $\text{O}1(t)\text{-Zn}1\text{-O}1(t)$ bridges.

Zunger.¹³ The integration over the Brillouin zone was performed using the Monkhorst–Pack scheme,¹⁴ with two k points.

To obtain the equilibrium lattice constant a_0 and bulk modulus B_0 , the energy versus the volume curve of each material was calculated allowing the atoms to relax at each volume, then each curve was fitted to the Birch–Murnaghan equation of state.¹⁵

III. RESULTS

Table I shows the equilibrium lattice constant and bulk modulus of all the compounds studied. Comparisons with experiments are only possible for Zn-IRMOF1, and the theoretical volume is 3% smaller than the experimental volume of desolvated Zn-IRMOF1.¹⁶ In the compounds studied the metal-atom nearest neighbor is always oxygen in the crystallographic position O1. Then, assuming that the atomic radii of O1 remains constant throughout all the compounds stud-

ied, one can obtain the relative size of the metal atom by looking at the distance to its closer neighbor. The distance between metal atoms and O1, $M\text{-O}1$, is tabulated in Table I. We interpret the change in this distance as Zn is replaced by other metal atoms to represent differences in their atomic radii. The calculated difference Δr in atomic radius relative to Zn is given in Table I. The quantity Δr allows us to make a correlation between the atomic radii M and the volume of *M*-IRMOF1, i.e., the bigger the atomic radii the larger the volume. This relation holds for metal atoms in the same column of the Periodic Table, but it does not hold if one considers different columns of the Periodic Table. For example, Mg and Zn have practically the same size, yet Mg-IRMOF1 has a larger volume than Zn-IRMOF1. In Table II the atomic positions of Zn-IRMOF1 are shown, and it is seen that the theoretical and experimental values are in excellent agreement.

To compare these compounds further, it is convenient to consider each one of them as made up of connectors and linkers. Table III contains structural information for the linker, and one observes that the linker remains practically unchanged throughout all the compounds. On the other hand,

TABLE I. Structural parameters of *M*-IRMOF1 ($M=\text{Zn}$, Cd, Be, Mg, and Ca). The equilibrium lattice constant a_0 and bulk modulus B_0 were obtained by fitting the energy vs the volume curve to the Birch–Murnaghan equation of state (Ref. 15). $M\text{-O}1$ represents the distance from the metal atom M to its closer neighbor, which is always oxygen in the crystallographic position O1. We interpret the change in this distance as Zn is replaced by other atoms to represent differences in their atomic radii. Δr represents the calculated difference in atomic radius relative to Zn (see text for an explanation).

Material	a_0 (Å)	B_0 (GPa)	$M\text{-O}1$ distance	
			(Å)	Δr (Å)
Zn-IRMOF1	25.6141 (25.8849 ^a)	17.955	1.913	0.0
Cd-IRMOF1	26.6125	14.890	2.115	-0.202
Be-IRMOF1	24.0089	21.103	1.602	0.311
Mg-IRMOF1	25.6670	15.657	1.903	0.01
Ca-IRMOF1	26.9418	12.262	2.125	-0.212

^aThe experimental a_0 was taken from the desolvated form of Zn-IRMOF1 (Ref. 16).

TABLE II. *Ab initio* and experimental (in parenthesis) atomic positions in fractional coordinates for Zn-IRMOF1. Space group $Fm\bar{3}m$. The experimental values were taken from the desolvated form of Zn-IRMOF1 (Ref. 16).

Atom type	Crystallographic position	x			y			z		
		x	y	z	x	y	z	x	y	z
H1	96k	0.191 (0.194)	0.191 (0.194)	0.049 (0.045)						
C3	96k	0.217 (0.218)	0.217 (0.218)	0.027 (0.026)						
C2	48g	0.054 (0.054)	0.250 (0.250)	0.250 (0.250)						
C1	48g	0.111 (0.112)	0.250 (0.250)	0.250 (0.250)						
O2	8c	0.250 (0.250)	0.250 (0.250)	0.250 (0.250)						
O1	96k	0.219 (0.219)	0.219 (0.219)	0.134 (0.134)						
Zn1	32f	0.207 (0.206)	0.207 (0.206)	0.207 (0.206)						

TABLE III. *Ab initio* structural parameters of the *linker* for each *M*-IRMOF1.

Material	C2-C3 (Å)	C1-C2 (Å)	C1-O1 (Å)	C3-C3 (Å)
Zn-IRMOF1	1.388	1.474	1.266	1.377
Cd-IRMOF1	1.386	1.469	1.264	1.373
Be-IRMOF1	1.388	1.468	1.262	1.377
Mg-IRMOF1	1.388	1.472	1.265	1.377
Ca-IRMOF1	1.389	1.476	1.266	1.377

Table IV shows significant differences among the connectors of different compounds. This is especially clear if one compares the volume of the connector in the different compounds; this volume was calculated assuming that the connector is an octahedron with vertices defined by the C1 atoms. In Table IV we have also collected the O1-*M* bond length and the O1-*M*-O1 bond angle, both variables are relevant for the following discussion on the electronic properties.

The electronic density of states and band structure of Zn-IRMOF1 are shown in Figs. 2(a) and 2(b), respectively. The top of the valence band is located at the Γ point, and the conduction band is split into two regions, the lower of which has a width of 138 meV. The bottom of the conduction band is very flat, making it impossible to unequivocally identify whether the band gap is direct or indirect. The band gap has a value of approximately 3.5 eV. Further inspection, obtained by calculating the partial electronic density of states shown in Fig. 2(c), reveals that the band-edge electronic states are overwhelmingly of a *p* nature. In particular, the bottom of the conduction band is dominated by *p* states contributed by the atoms O1, C1, C2, and C3 (the atoms of the linkers, although C1 and O1 are shared between linkers and connectors), whereas the top of the valence band is dominated by *p* states from O1, O2, C2, and C3.

TABLE IV. *Ab initio* structural parameters of the *connector* for each *M*-IRMOF1. The variable V_c stands for the volume of the connector assuming that it has an octahedral shape.

Material	M-O1 (Å)	O1-M-O1 (deg)	V_c (Å ³)
Zn-IRMOF1	1.913	107.011	59.600
Cd-IRMOF1	2.115	110.010	73.982
Be-IRMOF1	1.602	102.812	41.934
Mg-IRMOF1	1.903	108.210	60.495
Ca-IRMOF1	2.125	111.751	77.747

The electronic density of states and band structure of Be-IRMOF1 are shown in Figs. 2(d) and 2(e), respectively. Both are very similar to those of Zn-IRMOF1, the only clear difference, apart from the absence of *d* states, is that the lower part of the conduction band is wider, with a value 348 meV. After investigating the electronic density of states and band structure of the compounds Cd-IRMOF1, Mg-IRMOF1, and Ca-IRMOF1, we observed the following common features: A band-gap value of about 3.5 eV that is not unequivocally defined as direct or indirect, a band edge dominated by *p* states contributed by the same set of atoms, and a splitting of the conduction band into two bands, the lower of which has a width that varies. The band-gap values and the width of the lower part of the conduction band have been collected in Table V. We have also used the generalized gradient approximation¹⁷ (GGA) to compute the electronic properties of Zn-IRMOF1. We have found that neither the band gap nor the width of the lower part of the conduction band changes significantly. In particular, with GGA the band gap is 3.518 eV and the width is 131 meV. These results suggest that the features summarized above remain true independently of whether one uses the local or the generalized gradient approximation.

It is interesting to notice that, again if one focuses on the

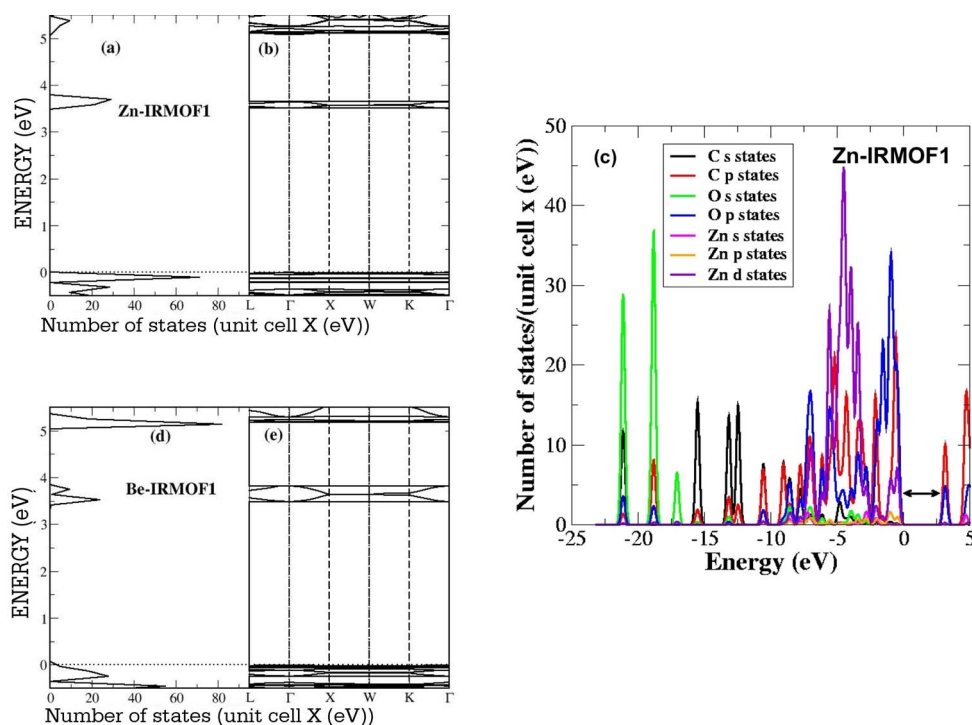


FIG. 2. Electronic properties of *M*-IRMOF1 (*M*=Zn and Be). (a) Electronic density of states, (b) electronic band structure, and (c) partial electronic density of states of Zn-IRMOF1; (d) electronic density of states and (e) electronic band structure of Be-IRMOF1. For clarity, only the region near the band gap is shown. The top of the valence band and Fermi level are located at 0.0. The Fermi level is indicated by the dotted line.

TABLE V. Electronic properties of *M*-IRMOF1. Electronic band gap and bandwidth of the lower part of the conduction band. (For aiding the text explanation, some of the structural parameters of the connectors have been also collected in the last two columns.)

Material	Band gap (eV)	Bandwidth (meV)	<i>M</i> -O1 (Å)	O1- <i>MO</i> 1 (deg)
Zn-IRMOF1	3.5027	138	1.913	107.011
Cd-IRMOF1	3.4885	81.2	2.115	110.010
Be-IRMOF1	3.4830	348	1.602	102.812
Mg-IRMOF1	3.5000	240	1.903	108.210
Ca-IRMOF1	3.5045	191	2.125	111.751

same column of the Periodic Table, one observes that there is a correlation between the width of the lower part of the conduction band of *M*-IRMOF1 and the size of *M*, i.e., the smaller the atomic radii of *M* the larger is the bandwidth of *M*-IRMOF1. To explain this correlation we notice the following three facts: First, the lower part of the conduction band is dominated by states contributed from the atoms of the linkers. Second, in the *M*-IRMOF1 structure, O1-*M*-O1 bridges join adjacent linkers. Third, a large bandwidth reflects enhanced interactions between the linkers. From Table V it is clear that, the smaller the atomic radii of *M* the smaller the length of the bridge O1-*M*-O1 and, as a consequence, the larger is the bandwidth. This is the reason why Be-IRMOF1 has the larger bandwidth followed by Mg-IRMOF1 and Ca-IRMOF1. Similarly, Zn-IRMOF1 has a larger bandwidth than Cd-IRMOF1. The same correlation does not hold if one compares the bandwidth of compounds made of metal atoms from different columns, though. For example, Zn and Mg have practically the same atomic radii, yet Mg-IRMOF1 has a larger bandwidth than Zn-IRMOF1.

The findings above suggest a possible path for tailoring the electronic properties of *M*-IRMOFs as to create materials with different metallic properties. This path consists of doping to raise the Fermi level up to the lower part of the conduction band, and then to take advantage of the tunability of the width of this band for creating materials with different metallic properties. For example, if this approach were to be successful and assuming that the bandwidths did not change significantly after doping, doped Zn-IRMOF1 should conduct less efficiently than doped Be-IRMOF1, since Be-IRMOF1 has a larger bandwidth than Zn-IRMOF1. In what follows we present results on Al and Li doping of Zn-IRMOF1 and Be-IRMOF1.

The formula unit of *M*-IRMOF is $H_{24}C_{48}O_{26}M_8$. To dope with Al, we replaced one Zn (Be) with one Al atom. The resulting material has one Al per unit cell and formula unit $H_{24}C_{48}O_{26}M_7Al$ ($M=Zn$ and Be). The materials $H_{24}C_{48}O_{26}Zn_7Al$ and $H_{24}C_{48}O_{26}Be_7Al$ were subsequently relaxed by means of a density-functional theory (DFT) technique that optimizes the volume and the atomic positions.¹⁰ The electronic densities of states of $H_{24}C_{48}O_{26}Zn_7Al$ and $H_{24}C_{48}O_{26}Be_7Al$ are shown in Figs. 3(a) and 3(b), respectively. In these figures, it can be seen that replacing Zn with Al results in shifting the Fermi energy up, so it lies now in what before was the lower part of the conduction band. Additionally, this band is wider in $H_{24}C_{48}O_{26}Be_7Al$ than in

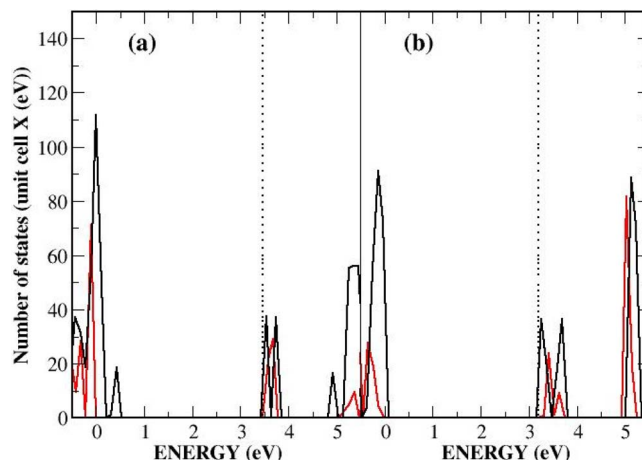


FIG. 3. Electronic properties of $H_{24}C_{48}O_{26}M_7Al$ ($M=Zn$ and Be). (a) Electronic densities of states of $H_{24}C_{48}O_{26}Zn_7Al$ (black line) and Zn-IRMOF1 (red line); (b) electronic densities of states of $H_{24}C_{48}O_{26}Be_7Al$ (black line) and Be-IRMOF1 (red line). For clarity, only the region near the band gap is shown. The Fermi level for $H_{24}C_{48}O_{26}M_7Al$ ($M=Zn$ and Be) is indicated by the black dotted line.

$H_{24}C_{48}O_{26}Zn_7Al$. So it appears that Al doping in *M*-IRMOF1 could be a successful approach for creating *M*-IRMOF materials with different metallic properties. However, it should be noted that Al doping introduces other changes in the electronic density of states. For example, changes in the heights and splitting of the peaks are observed with Al doping (see Fig. 3).

Adding one Li atom per unit cell results in the material $H_{24}C_{48}O_{26}M_8Li$, which represents the case of Li doping. To find the most likely position a Li atom would occupy, we initially performed classical molecular mechanics and semi-empirical quantum modeling. We first determined a minimum-energy position of a Li atom using classical valence force fields [molecular mechanics 3 (MM3) and optimized potentials for liquid simulations (OPLS)] (Ref. 18) followed by geometry optimization using a semiempirical calculation based on Modified Neglect of Diatomic Overlap with inclusion of *d*-orbitals MDNO(*d*).¹⁹ These relatively low-level calculations gave results showing that the Li is attracted to the connector, occupying a position between two O1 atoms and very close to Zn (Be). Limited quantum mechanics (QM)/MM modeling was also used to allow implementing of a higher level of many-body electronic structure. In this case, the Li atom and the connector (atoms giving *sp*³ termination) were treated within the Hartree-Fock [all electron model with Slater-type orbital (STO)-3G* atom centered basis functions] with single-point second-order perturbation corrections for electron correlation, and the remaining atoms of the *M*-IRMOF1 were treated with MM3. Subsequently, we relaxed $H_{24}C_{48}O_{26}Zn_8Li$ and $H_{24}C_{48}O_{26}Be_8$ by means of a DFT technique in the following manner: (i) We relaxed both volume and atomic positions and (ii) we relaxed the atomic positions only. In either case we observed large structural changes introduced by doping with Li. This indicates that adding Li to IRMOFs does more than simply raising the Fermi level without altering much the electronic properties of IRMOFs, as we originally speculated. Therefore, Li dop-

ing does not appear to be a suitable approach for producing IRMOFs with different metallic properties by taking advantage of the different conduction bandwidths.

IV. CONCLUSIONS

In this paper we have investigated the possibility of tailoring the electronic properties of isorecticular metal-organic framework 1 (IRMOF1). The electronic properties of this material can be altered by changing the connector, the linker, or both. We investigated by changing the connector, in particular, we replaced the Zn atoms by other metal atoms and examined the electronic properties of *M*-IRMOF1 (*M*=Be, Mg, Ca, Zn, and Cd) by means of an *ab initio* electronic structure method. Our results show that all these compounds share a similar but relatively large band gap of about 3.5 eV, and that their conduction band is divided into two parts, the lower of which has a width that varies with metal substitution. This variation in the bandwidth can be qualitatively explained as due to a size effect introduced by the metal atom: The smaller the metal, the closer the linkers which results in a larger bandwidth. This finding leads us to consider the possibility of doping to raise the Fermi level up to the lower part of the conduction band, so one could take advantage of different bandwidths to create materials with different metallic properties. We investigated the electronic properties of Al- and Li-doped Zn-IRMOF1 and Be-IRMOF1, and found that Al doping could be a successful approach to create *M*-IRMOF1 with different metallic properties, whereas Li doping is not. The latter is due to significant structural changes introduced by the addition of Li. The potential for tailoring the electronic properties of *M*-IRMOF1 becomes apparent when one realizes that this material is just one among 16 other IRMOFs, which have the same connector but different linkers. The possibility of changing linkers, connectors, or both, and even replacing Zn with magnetic elements, plus doping, could offer an interesting venue for the creation of materials with interesting electronic and magnetic properties.

ACKNOWLEDGMENTS

We would like to thank Professor M. O'Keeffe, who suggested to us that Be-IRMOF1 and Mg-IRMOF1 could possibly exist. Also, we would like to thank Professor O. M. Yaghi for kindly reporting to us that his group had synthesized many new IRMOFs with different metal atoms, including Co and Cd. This research has been supported by the Director, Office of Science, Office of Basic Energy Sciences, U.S. Department of Energy, and used the resources of the National Center for Computational Sciences at Oak Ridge National Laboratory, which is supported by the Office of Science of the Department of Energy under Contract No. DE-AC05-00OR22725 with UT-Battelle.

- ¹J. C. L. Rowsell, A. R. Millward, K. S. Park, and O. M. Yaghi, *J. Am. Chem. Soc.* **126**, 5666 (2004).
- ²N. L. Rosi, J. Eckert, M. Eddaoudi, D. T. Vodak, J. Kim, M. O'Keeffe, and O. M. Yaghi, *Science* **300**, 1127 (2003).
- ³M. Eddaoudi, J. Kim, N. Rosi, D. Vodak, J. Wachter, M. O'Keeffe, and O. M. Yaghi, *Science* **295**, 469 (2002).
- ⁴G. J. Halder, C. J. Kepert, B. Moubaraki, K. S. Murray, and J. D. Cashion, *Science* **298**, 1762 (2002).
- ⁵S. Stepanow, M. Lingenfelder, A. Dmitriev *et al.*, *Nat. Mater.* **3**, 229 (2004).
- ⁶M. A. Lingenfelder, H. Spillmann, A. Dmitriev, S. Stepanow, N. Lin, J. V. Barth, and K. Kern, *Chem.-Eur. J.* **10**, 1913 (2004).
- ⁷J. S. Seo, D. Whang, H. Lee, S. I. Jun, J. Oh, Y. J. Jeon, and K. Kim, *Nature (London)* **404**, 982 (2000).
- ⁸W. Bragg and G. T. Morgan, *Proc. R. Soc. London, Ser. A* **104**, 437 (1923).
- ⁹A. B. Blake, *Chem. Commun. (London)* **16**, 5691966.
- ¹⁰G. Kresse and J. Hafner, *Phys. Rev. B* **47**, RC558 (1993); G. Kresse, Ph.D. thesis, Technische Universität Wien, 1993; G. Kresse and J. Furthmüller, *Comput. Mater. Sci.* **6**, 15 (1996); G. Kresse and J. Furthmüller, *Phys. Rev. B* **54**, 11169 (1996).
- ¹¹D. Vanderbilt, *Phys. Rev. B* **41**, 7892 (1990).
- ¹²D. M. Ceperly and B. J. Alder, *Phys. Rev. Lett.* **45**, 566 (1980).
- ¹³J. Perdew and A. Zunger, *Phys. Rev. B* **23**, 5048 (1981).
- ¹⁴H. J. Monkhorst and J. D. Pack, *Phys. Rev. B* **13**, 5189 (1976).
- ¹⁵F. Birch, *J. Geophys. Res.* **57**, 227 (1952).
- ¹⁶H. Li, M. Eddaoudi, M. O'Keeffe, and O. M. Yaghi, *Nature (London)* **402**, 276 (1999).
- ¹⁷J. Perdew, *Electron Structure of Solids*, edited by P. Ziesche and H. Escrig (Akademie, Berlin, 1991).
- ¹⁸N. L. Allinger, Y. H. Yuh, and J. H. Lii, *J. Am. Chem. Soc.* **111**, 8551 (1989); N. L. Allinger, X. Zhou, and J. Bergsma, *J. Mol. Struct.: THEOCHEM* **312**, 69 (1994).
- ¹⁹W. Thiel and A. A. Voityuk, *J. Phys. Chem.* **100**, 616 (1996); W. Thiel, *Adv. Chem. Phys.* **93**, 703 (1996).